



Levan Production by *Paenibacillus polymyxa* Immobilized on $\text{Fe}_3\text{O}_4@SiO_2$ Nanoparticles Using Molasses Medium with Emphasis on the Bioactivity

Gözde Koşarsoy Ağçeli¹ · Hande Günan Yücel²

Accepted: 6 June 2023 / Published online: 30 June 2023

© The Author(s), under exclusive licence to Springer Science+Business Media, LLC, part of Springer Nature 2023

Abstract

In this study, levan biopolymer (a fructose-based exopolysaccharide) was produced by *Paenibacillus polymyxa* HCT33-3, which was immobilized onto the composite of silica-coated magnetite nanoparticles ($\text{Fe}_3\text{O}_4@SiO_2$ NPs). For this purpose, firstly, synthesis of magnetite nanoparticles (Fe_3O_4 NPs) was followed by $\text{Fe}_3\text{O}_4@SiO_2$ composite formation to enhance its stability. The characterization studies were investigated with the scanning electron microscopy and energy dispersive X-ray analyzes, transmission electron microscopy, X-ray diffraction analyses. Then, the microorganism *Paenibacillus polymyxa* HCT33-3, immobilized onto $\text{Fe}_3\text{O}_4@SiO_2$ and levan fermentation was carried out in the media including molasses. Effects of molasses percentage in the growth media, initial pH, temperature and fermentation period parameters were tested on levan production capability. The highest levan concentration of 35.8 g/L was obtained at the 54th hour in the medium including 20% molasses (v/v) with the initial pH and temperature values of 7.0 and 37 °C, respectively. The characterization studies clearly confirmed that the produced exopolysaccharide was levan, which showed an antimicrobial effect against all microorganisms used in the study, besides its effectiveness on the biofilm formed by *Pseudomonas aeruginosa*. This is the first study focusing on high-value levan biopolymer production by the immobilized microorganisms onto $\text{Fe}_3\text{O}_4@SiO_2$ nanocomposite in the growth media including molasses as the sole carbon source. This environmentally friendly process, which can potentially enable the repeated use of the cells, seemed to be significantly advantageous in terms of both cost and sustainability.

Keywords Bioactivity · Levan · Magnetite nanoparticles · Molasses · *Paenibacillus polymyxa* · Silica-coated

Introduction

Levan is a polymeric structure that can be obtained from certain plant species, Archaea or produced by some microorganisms. It is fructose biopolymer predominantly linked by β -2,6 glycosidic 6 + bonds and β -2,1-linked side chains [1]. In addition to being a limited plant species that produce levan, a much wider variety of microorganisms perform the production of levan. Microbial levan production is carried out by various microorganisms such as *Bacillus subtilis*, *Bacillus polymyxa*, *Aerobacter levanicum*, *Streptococcus*

sp., *Pseudomonas* sp., *Corynebacterium laevaniformans*, *Zymomonas mobilis*, *Brachy bacterium phenoliresistens*, *Erwinia*, *Azotobacter* in production environments containing sucrose [2–5].

Levans are fructose-based polysaccharides with a variety of potential applications in a variety of industries such as food, cosmetics, pharmaceuticals, and medical [6–8]. Levan and levan-type fructooligosaccharides have been found to have positive effects on human and animal intestinal microbiota and probiotic microorganisms. Adamberg et al. reported an increase in the microbiota of *Bacteroides*, *Escherichia*, *Streptococcus* and *Faecalibacterium* due to the use of levan in human stool samples that they analyzed using metagenomic and metabolomic methods [9]. Levan-based films are used in biodegradable food packaging with a good oxygen barrier [7, 10]. One of the most exciting research in the medical field is the production of levan-based thin films to heal damaged tissue. According to Sturzoiu et al., levan plays a role in activating metalloproteinases, which

✉ Gözde Koşarsoy Ağçeli
gozdekosarsoy@gmail.com

¹ Department of Biology, Faculty of Science, Hacettepe University, 06800 Ankara, Turkey

² Chemical Engineering Department, Faculty of Engineering, Hacettepe University, 06800 Ankara, Turkey

is a crucial step in the healing of burned or mechanically damaged tissues [11]. Furthermore, the antimicrobial and antibiofilm properties of levan are highly significant in medical applications in our current era where antibiotic-resistant microorganisms are increasing [12–14]. Although the mechanism of the antimicrobial and antibiofilm effect of levan is not yet fully known, it has been reported that this may be due to changes in the cell surface that reduce auto-aggregation and bacterial cell interaction as well as inhibition of the adhesion mechanism in the early stages of bacterial growth [14, 15].

It would be very advantageous in terms of the process cost when waste and by-products are used as a nutrient medium for the cells during the microbial production process of levan, which is a quite promising biopolymer for future applications. Syrups and molasses are the most common sucrose sources used for this purpose in fermentative production [16]. Molasses is a dark brown and viscous liquid byproduct produced during the formation process of sugar crystals using repeated evaporation, centrifugation, and crystallization methods from sugar beets or cane juices. It has a weak fluidity and is considered a byproduct of the sugar-making process [17]. Molasses, which consists of 23–26% water, 47–48% sugar, 9–14% mineral substances (Mg, Mn, Al, Fe and Zn) and 8–12% nitrogenous compounds, significantly increases microbial growth efficiency due to its rich nutritional content [18, 19]. Bio-products and industrial enzymes with high added value such as bioethanol, single cell oil (SCO), pullulan, fructooligosaccharides (FOS), polysaccharides, lipase, protease can be produced by microorganisms through different biosynthetic pathways by using molasses [20–22].

Nanoparticles (NPs), which are particles having dimensions of 100 nm and below, show superior properties (i.e., quantum size effects, size dependence of its electronic structure, unique characteristics of surface atoms, and high surface-to-volume ratio) when compared to many of the commercial materials. Magnetic NPs are widely used in magnetic fluids, catalysis, biotechnology, biomedicine, magnetic resonance imaging, information storage, environmental remediation [23]. The ability of magnetic NPs (MNPs) to be moved by applying magnetic field provides advantages in many application areas, especially in the medicine [24]. MNPs are one of the most used nanomaterials in disease diagnosis, targeted drug delivery, and biomedical imaging, such as magnetic resonance imaging (MRI) [25]. MNPs have a wide range of uses in cancer treatments as they can combine multiple functions [26]. Thanks to its large surface area, metal nanoparticles enable to transport large amounts

of drugs and medical cargoes in drug delivery applications [27–29].

Magnetite (Fe_3O_4) is one of the most widely used magnetic NP structure. It has a cubic structure formed on an inverted backbone. While the oxygen atoms forming this structure are arranged facing the center, the Fe cations are surrounded by 4 or 6 oxygen atoms [30]. Electrons show transition property between Fe^{2+} and Fe^{3+} ions at the room temperature, so it is a semi-metallic material. In different studies, the encapsulation of Fe_3O_4 NPs can be done with various compounds such as TiO_2 , ZrO_2 , SiO_2 . The use of silica, among these, is very advantageous due to its non-toxicity, transparency, stability of biocompatibility at different pH and temperatures, and prevention of NP leakage. In addition, immobilization of structures such as microorganisms and enzymes on silica-coated iron oxide NPs and their applications are among the new research topics [31–35].

Levan can be produced by immobilizing the levansucrase enzyme on titanium-activated magnetite [36]. Microbial bioreactors can be developed by immobilizing microorganisms into nanoparticles [23]. If a microbial cell is immobilized in the magnetite, it can be directed to an exact target easily. Therefore, the transport of the substances such as enzymes and polymers, which will be produced by the microorganism trapped in the magnetic nanoparticle, would be possible by applying magnetic field. However, there is no report revealing with levan production from enzymes or microorganisms immobilized on silica coated magnetite.

Considering the usage areas of magnetite nanoparticles, it was concluded that these particles can also play a role in biopolymer production. In this context, several questions arose in our minds: How will the entrapment of microorganisms with levansucrase enzyme into these nanoparticles affect the yield in levan production? Is it possible to obtain levan from microorganisms that are trapped in nanoparticles in molasses medium? What is the bioactivity of the levan obtained with the immobilized microorganisms? Silica-coated magnetite ($\text{Fe}_3\text{O}_4@\text{SiO}_2$) nanoparticles were immobilized with *Pae-nibacillus polymyxa HCT33-3* to produce levan in molasses media, in order to search for answers to all of these questions. The conditions affecting levan production efficiency, such as pH and temperature, were examined, and the bioactivity of the obtained levan was evaluated (Fig. 1). This is the first study in which levan production was performed by immobilizing a microorganism on $\text{Fe}_3\text{O}_4@\text{SiO}_2$ nanoparticles in a culture medium using molasses as a carbon source. In addition to the repeated usability potential of the bacteria immobilized on nanoparticles, the valorization of molasses for the bioproduction of such a valuable polymer having wide variety of applications will provide new ideas for future research.

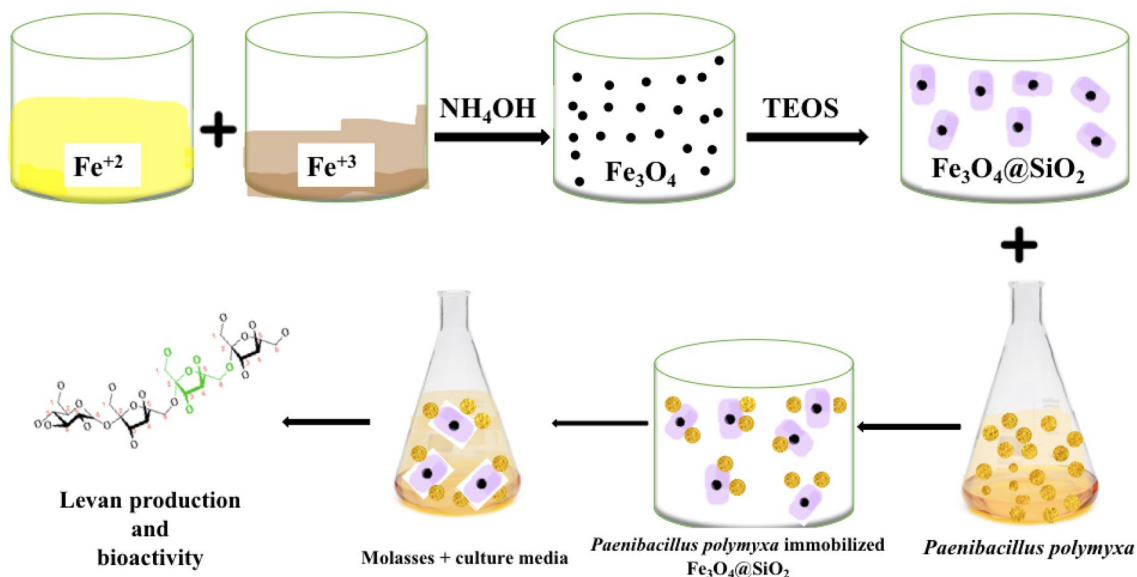


Fig. 1 Production of levan biopolymer in molasses medium from *Paenibacillus polymyxa* immobilized on $\text{Fe}_3\text{O}_4@/\text{SiO}_2$ nanoparticles and determination of the bioactivity of the produced levan

Materials and Methods

Materials and Bacterial Culture

Paenibacillus polymyxa HCT33-3 culture, which was isolated from previous studies and known to produce levan, was obtained from Hacettepe University, Department of Biotechnology (Ankara, Turkey). *P. polymyxa* HCT33-3 has levan-sucrase enzyme at a concentration of > 5 U/mL. NH_4OH , $\text{FeCl}_3 \cdot 6\text{H}_2\text{O}$, $\text{FeCl}_2 \cdot 4\text{H}_2\text{O}$, Tetraethyl orthosilicate (TEOS) and all other chemicals and media used were obtained from Sigma-Aldrich (Merck). Molasses was obtained from RCan Ticaret (Turkey). The molasses content used in the medium is listed as follows; 73–79% dry matter, 48–57% Sucrose, 11–12% Protein, 1.3% Specific Gravity, 8–10% Crude Ash, 2–2.7% Invert Sugar, Arsenic mg/kg up to 1, Copper mg/kg up to 18, Zinc mg/kg up to 100, Iron mg/kg up to 100, Tin mg/kg up to 100, Lead mg/kg up to 2, 80–83 Brix (total dissolved matter), 0.2–0.5% Calcium, 0.05–0.3% Phosphorus, 1% Sodium [37].

Methods

Synthesis and Characterization of Fe_3O_4 NPs

50 mL of NH_4OH was added to 200 mL deionized water and mixed at 1000 rpm. 2.5 mmol of $\text{FeCl}_3 \cdot 6\text{H}_2\text{O}$ and 1.25 mmol of $\text{FeCl}_2 \cdot 4\text{H}_2\text{O}$ were separately dissolved in 50 mL of distilled water to prepare a 0.5 mol solution. 10 mL of FeCl_2 and 20 mL of FeCl_3 solutions were added to the NH_4OH

solution. The mixture was stirred at 100 rpm for 2.5 min, until a black precipitate was observed. The resulting precipitate was washed four times with deionized water and Fe_3O_4 NPs were magnetically separated. The structural and surface properties of the produced NPs were investigated.

Encapsulation of Fe_3O_4 NPs Through Silica

2 g of Fe_3O_4 NPs were dispersed in Millipore water and this mixture was placed in a solution containing ethanol (80 mL) and water (40 mL). 3 mL of ammonium hydroxide (NH_4OH) and 2 mL of tetraethyl orthosilicate (TEOS) were added to this mixture and stirred for 24 h. The precipitate obtained was separated, washed three times with Millipore water and dried in an oven at 80 °C. The untreated Fe_3O_4 NPs and the silica encapsulated composite ones ($\text{Fe}_3\text{O}_4@/\text{SiO}_2$) were characterized comparatively.

Immobilization of the Microorganism

Paenibacillus polymyxa HCT33-3 colonies were inoculated in 5 mL of TSB (Tryptone Soy Broth) and allowed to grow overnight. The concentration of *Paenibacillus polymyxa* HCT33-3 cultures in the initial inoculum was 5.0×10^6 CFU/mL. Then, 200 μL of culture was transferred to 20 mL of TSB and incubated at 37 °C for 24 h. Bacteria were separated from the culture media by centrifugation at 9000 rpm for 20 min. 20 mg of $\text{Fe}_3\text{O}_4@/\text{SiO}_2$ nanocomposite was dispersed in 5 mL of bacteria suspension. To immobilize the bacteria on the magnetic nanocomposite, the mixture was stirred in an incubator at 150 rpm and 37 °C for 30 min. The precipitate was washed

three times with distilled water to remove the free cells and the growth media constituents. The morphologies of the immobilized cells were visualized via microscopic techniques.

Production and Characterization of Levan

Levan was produced in sterile nutrient media including molasses at varying ratios between 1.5 and 50% (v/v) in addition to 1.0 g/L K_2HPO_4 , 1.0 g/L $(NH_4)_2SO_4$ and 0.5 g/L $MgSO_4 \cdot 7H_2O$. Effects of initial sugar concentration, pH, temperature and time on levan production efficiencies were investigated. Each culture was inoculated at 1 McFarland standard at 10% (v/v) and incubated at 37 °C for 48 h. The media were centrifuged at 4000 rpm for 15 min and the immobilized cells were separated from the liquid phase. The polymers were precipitated by adding ethanol at a ratio of 1:2 (v/v) to the supernatants, whose pH was adjusted to 10.0. Then, the levan particles were collected after centrifugation of the mixture at 4000 rpm for 10 min and removal of the ethanol. The precipitated levan biopolymer was dissolved in distilled water at 4 °C. Levan solution was dialyzed against distilled water (MWCO 14,000 Da) for 24 h. Levan was precipitated again with ethanol and centrifuged at 10,000 rpm for twenty minutes. The pure levan obtained was dried in an oven at 45 °C and weighted [38]. The same procedure was applied to the non-immobilized *Paenibacillus polymyxa* HCT33-3 and levan production was carried out. This experiment was carried out in three repetitions. The levan produced at the optimum condition was stored for further analysis (FTIR, NMR and XRD) in tightly closed containers.

Calculation of Levan Production Efficiency

The percentage ratio of the produced levan (product) concentration and consumed sucrose (substrate) concentration at any experimental condition was defined as “conversion efficiency” (Eq. 1).

$$\text{Conversion Efficiency (\%)} = \frac{P}{S_0 - S} \quad (1)$$

Here P: Product (levan) concentration (g/L), S_0 : Initial substrate (sucrose) concentration (g/L), S: Substrate (sucrose) concentration at time t (g/L).

The product yield was also calculated in terms of initial substrate concentration and expressed as “Effective efficiency” (Eq. 2).

$$\text{Effective Efficiency} = P/S_0 \quad (2)$$

Analytical Methods

Initial reducing sugar concentrations of the growth media were determined spectrophotometrically (Shimadzu UV-1700, Kyoto, Japan) with DNS (3-5 Dinitrosalicylic acid) method [39]. 0.1 g of levan powder was dissolved in 0.1 N HCl at 100 °C for an hour. After the levan hydrolysis, 1 mL of freshly prepared DNS was added to two test tubes. One of the test tubes contained 1 mL of the hydrolyzed levan sample, and the second test tube contained 1 mL of distilled water as a blank. The test tubes were then placed in a water bath container for 10 min and allowed to cool to ambient temperature. To obtain an appropriate dilution from the sample, 10 mL of distilled water were added to each individual tube. Standard solutions containing 0.09, 0.18, 0.27, and 0.36 mg/mL of fructose were prepared using this method. Measurements were then taken using a spectrophotometer at a wavelength of 575 nm [40]. Total concentrations of the unconsumed sugars remaining in the nutrient media were measured using Phenol–Sulphuric Acid method [41]. 50 μ L sample of levan at a concentration of 1 mg/mL was mixed with 100 μ L of concentrated sulfuric acid solution (75% v/v). Then, 200 μ L of anthrone reagent, which consisted of 5 mg of anthrone dissolved in 100 μ L of ethanol and mixed with 2.4 mL of 75% v/v sulfuric acid, was added to the mixture. The resulting mixture was incubated at 100 °C for 15 min in a dry oven. After heating, the mixture was allowed to cool for 5 min at room temperature. To analyze the levan samples, standard solutions containing sucrose at concentrations of 20, 40, 60, 80, and 100 mg/L were prepared. The cooled levan samples and the standard solutions were read on a spectrophotometer at a wavelength of 490 nm [14, 42]. The functional groups included in the NPs, nanocomposites and biopolymer were analyzed using Fourier Transform Infrared Spectrophotometer (FTIR) (Thermo Scientific Nicolet 6700 Smart iTR). FTIR spectra were recorded in the range 4000–400 cm^{-1} [43]. The scanning electron microscopy and energy dispersive X-ray analyzes (SEM/EDX) (Tescan, GAIA3 + Oxford XMax 150 EDS) showed the surface morphologies and/or elemental compositions of the particles and composites. For SEM/EDX analysis, the samples were coated with an Au sputtering layer [44]. Size and shape of the untreated and silica-coated NPs were evaluated by using transmission electron microscopy (TEM) (FEI 120 kV HCTEM) [45]. To prepare samples for TEM analysis, a drop of diluted solution was deposited on an amorphous carbon-coated copper grid. Low-resolution images were captured using a FEI 120 kV HCTEM microscope operating at 120 kV [46]. 1H and ^{13}C nuclear magnetic resonance (NMR) (Bruker \mathcal{C} 300, 400 MHz) spectra analyzes were carried out for levan fermented. Each sample for 1H and ^{13}C NMR analysis contained 0.5 mg of levan, which was dissolved in dimethylsulfoxide (DMSO). The 1H NMR

spectra were collected using a 300 MHz instrument, while the ^{13}C NMR spectra were collected using a 75.46 MHz instrument [5]. X-ray diffraction (XRD) analysis were performed by using Rigaku Ultima IV Diffractometer under a $\text{Cu K}\alpha$ radiation at 40 kV/30 and with a scan rate of 1 deg/min [47].

Determination of Bioactivity of Levan

Evaluation of Antimicrobial Effect of Levan by Agar Diffusion Test

Different concentrations of levan (0.50 g/mL, 0.25 g/mL, 0.10 g/mL) from immobilized *Paenibacillus polymyxa* HCT33-3, pure levan (0.50 g/mL) from *Erwinia herbicola* (Sigma) and 0.5 g/mL levan from unimmobilized *Paenibacillus polymyxa* were dissolved in 1 mL of distilled water and absorbed into the empty antibiotic discs.

In order to observe the antimicrobial effect, 0.5 McFarland, 100 μL of bacteria were inoculated on Mueller–Hinton Agar. 0.5 McFarland, 100 μL of *Candida albicans* was inoculated on Sabouraud Dextrose Agar. 100 μL (10^5 spores/mL) of *Aspergillus niger* was inoculated on Sabouraud Dextrose Agar. After spreading *E. coli* ATCC 35218, *Staphylococcus aureus* subsp. *aureus* ATCC@29213TM, *Klebsiella pneumoniae* ATCC 1705, *Pseudomonas aeruginosa* ATCC 27853 as bacteria, *Candida albicans* ATCC® 90029TM as yeast, and *Aspergillus niger* as mold on Petri dishes, discs impregnated with levan were placed on petri dishes under sterile conditions and the antimicrobial effect was determined by measuring zone diameters by digital caliper (Insize 1108-150 Digital caliper). The experiment was repeated three times.

Evaluation of Antimicrobial Effect of Levan by Minimum Inhibitory Concentration (MIC)

Minimum inhibitory concentration (MIC) test of levan produced from *Paenibacillus polymyxa* HCT33-3 was determined by standard method E2149-13a from the American Society for Testing and Materials (ASTM) [48]. *E. coli* ATCC 35218, *Staphylococcus aureus* subsp. *aureus* ATCC@29213TM, *Klebsiella pneumoniae* ATCC 1705, *Pseudomonas aeruginosa* ATCC 27853 were used as bacterial cultures and *Candida albicans* ATCC® 90029TM as the yeast culture. In this analysis, bacterial and yeast suspensions were prepared at a concentration of $\sim 10^6$ CFU/mL (0.5 McFarland). For *Aspergillus niger*, the measurement of spore count was performed on the Thoma slide (Merck) where the fungal concentration was adjusted to 10^5 spores/mL. For bacterial culture, 1 mL of each bacterial suspension was added to 9 mL of Luria Broth medium. For fungal culture, 1 mL of *Candida* and *Aspergillus* cultures were added to 9 mL of Sabouraud Dextrose Broth medium. Levan

solutions obtained from *Paenibacillus polymyxa* HCT33-3 at concentrations of 0.5 g/mL, 0.25 g/mL, 0.10 g/mL, pure levan solution (0.5 g/mL) obtained from *Erwinia herbicola* and 0.5 g/mL concentrations of levan by untreated *Paenibacillus polymyxa* HCT33-3 1 mL was added to each medium. Bacteria were incubated at 37 °C for 24 h, fungi at 30 °C for 48 h and microbial concentrations, measured as absorbance at a wavelength of 600 nm. Control experiments were also performed without levan biopolymer solutions. The experiment was repeated 3 times and the results were compared with the control groups [49, 50].

Antibiofilm Effect

Within the scope of the study, biofilm formations were investigated by “Crystal Violet Stained Biofilm Measurement on Plate”. The *Pseudomonas aeruginosa* strain, known to produce biofilm, was inoculated into Brain Heart Infusion Broth medium in accordance with the McFarland 2.0 (6×10^8 CFU/mL) standard and left for a 24-h incubation at 37 °C. After 24 h, the samples were diluted 1:100 and 1 mL of each were transferred to the wells of a 24-well polystyrene plate under sterile conditions. 0.5 g/mL levan solution (from untreated cells), pure levan (0.50 g/mL) from *Erwinia herbicola* (Sigma) and different concentrations (0.50 g/mL, 0.25 g/mL, 0.10 g/mL) of levan solutions (from immobilized cells) were added to each well. After the samples were loaded into the wells, the plate was closed and incubated at 37 °C. Plates, after a certain incubation period, were removed from the incubator. The liquid cultures on the plate were taken from the plate medium and the wells were washed with distilled water so that no culture residues remained. After the washing process was completed, the plates were allowed to dry. After the plate dried, 1% Crystal Violet solution was added to the wells and waited for 40–45 min for staining. 1 mL of Ethanol-Acetic Acid (90:10) solution was added to the wells and the Crystal Violet solution was dissolved. The amount of Crystal Violet dissolved in the Ethanol-Acetic Acid solution was determined by measuring in a spectrophotometer device at 540 nm, and the effect of the obtained levan on the biofilm was evaluated in this way. The experiment was repeated 3 times.

Results and Discussion

Characterization of Untreated and Silica coated Fe_3O_4 Nanoparticles

FTIR

A composite structure ($\text{Fe}_3\text{O}_4@ \text{SiO}_2$) was obtained by coating the produced magnetite NPs with silica. FTIR analysis

of both samples was performed to compare the structural changes in the particles after the silica coating process and the results were presented in Fig. 2. The peak observed at 542 cm^{-1} in magnetite NP is due to the stretching vibration in the Fe–O metal–oxygen bond, which is very characteristic for this particle [51]. The peaks seen around 1991, 1505, 1318 and 1094 cm^{-1} were related with deionized water used as solvent [52]. The FTIR spectrum of $\text{Fe}_3\text{O}_4@\text{SiO}_2$ composite significantly differed from that of the untreated NPs. While the large peak observed at 1031 cm^{-1} indicated the presence of asymmetrical –Si–O–Si– bond stretching; another characteristic peaks seen at 783 cm^{-1} and 948 cm^{-1} revealed the symmetrical bond stretching and stretching vibration of –Si–O–Si– bond, respectively. The peak at 576 cm^{-1} was related with Fe–O stretching vibration, which indicated the presence of ferrous oxide structure [53]. Hence, the FTIR spectra obtained for the untreated and silica coated magnetite particles, which were found to be quite compatible with the literature data, showed the efficiently produced $\text{Fe}_3\text{O}_4@\text{SiO}_2$ composite material.

SEM/EDX

The effect of silica coating on surface characteristics of magnetite NPs were investigated via SEM/EDX analysis (Fig. 3). The results reveal the regular morphologies of untreated magnetite particles, which include high levels of Fe and O elements (Fig. 3a). SEM micrographs of silica coated magnetite particles clearly showed the increase in the particle size in addition to their uniform structure (Fig. 3b). Elemental analysis also showed that there was a significant increase in the ratio of O element in addition to the existing Fe element found in the NPs. The existence of the Si element was also an indicator showing efficient interaction between magnetite NPs and silica.

TEM

Particle dimensions and detailed surface characteristics were investigated with TEM. The results confirmed the SEM images. The magnetite NPs were found to be having diameter values around 10 nm. The significant increase in the particle size clearly indicated the change on the magnetite surface which was caused by its coating with silica (Fig. 4).

XRD

XRD diagram of silica coated magnetite NPs ($\text{Fe}_3\text{O}_4@\text{SiO}_2$) was shown in Fig. 5. The main peaks obtained at 30.2° , 35.7° , 43.7° , 54.2° , 57.6° and 63.1° are the characteristic peaks of (220), (311), (400), (422), (511), and (440) crystalline planes of magnetite nanoparticles, respectively [54, 55]. In addition, the broad peak seen at 22.7° confirms the presence of amorphous silica in the nano-composite produced [56].

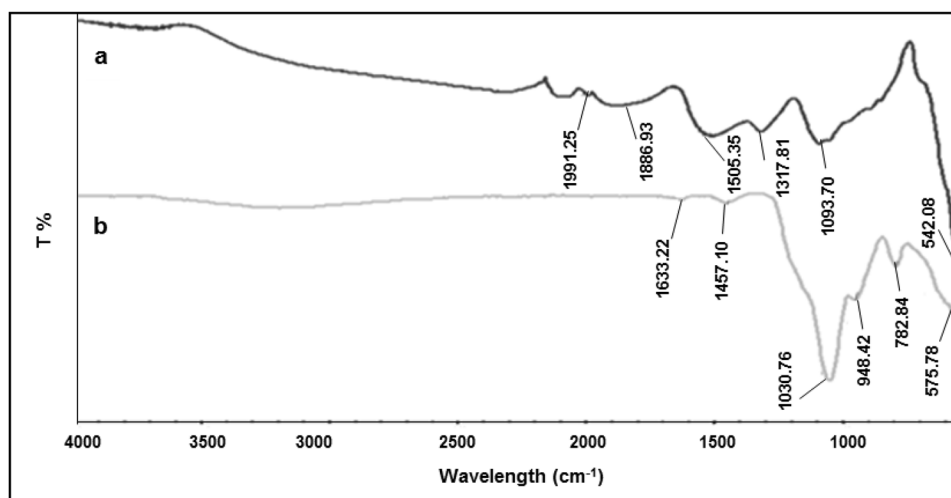
Characterization of Microorganism- $\text{Fe}_3\text{O}_4@\text{SiO}_2$ Composite

Surface characterization of the composite structure, which was obtained with the immobilization of cells onto silica-coated magnetite NPs (Microorganism + $\text{Fe}_3\text{O}_4@\text{SiO}_2$), was carried out with SEM (Fig. 6) analysis. The images demonstrated the presence of cellular structures in the composite and hence, successfully carried out immobilization process.

Levan Production

Effects of molasses ratio in the growth media, initial pH, temperature and time on levan concentration were shown in Fig. 7.

Fig. 2 FTIR spectra for (a) untreated magnetite NPs, (b) silica-coated magnetite NPs ($\text{Fe}_3\text{O}_4@\text{SiO}_2$)



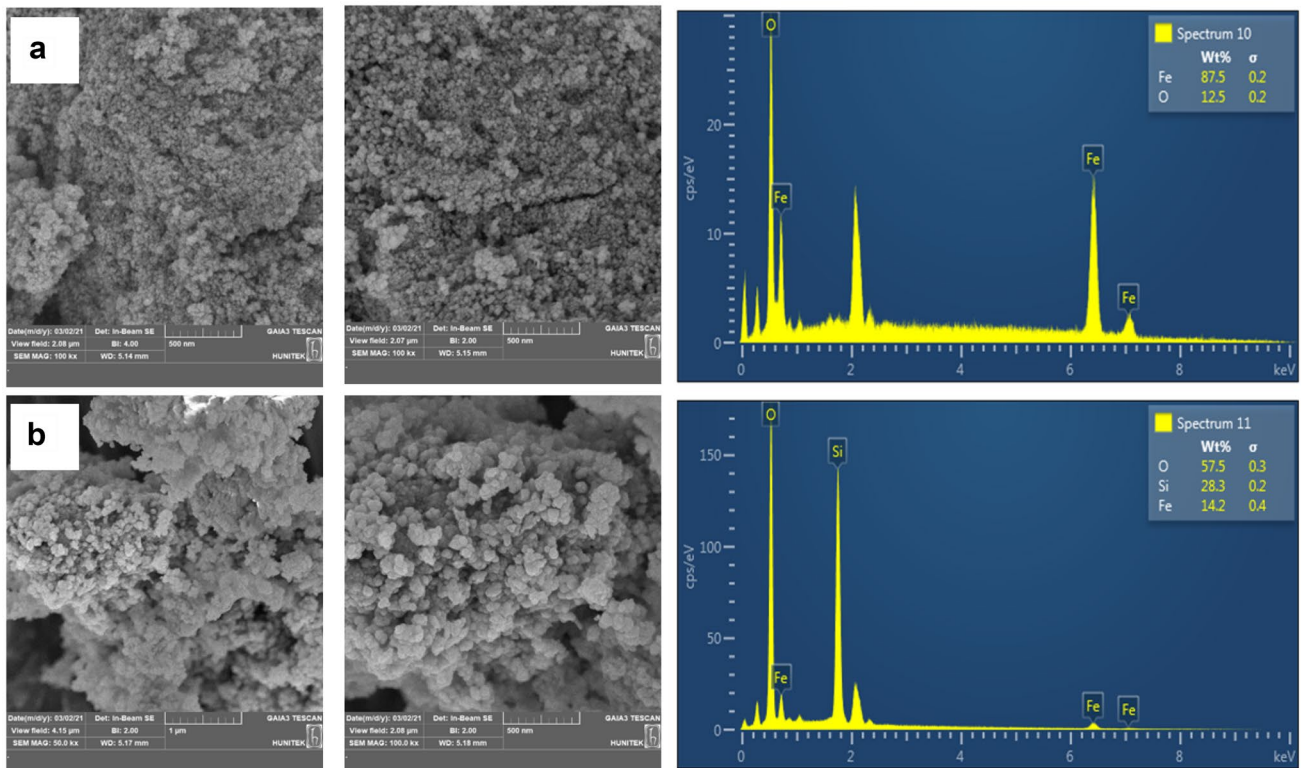


Fig. 3 SEM/EDX micrographs of **a** untreated magnetite NPs (magnification of 100 kx) and **b** silica coated magnetite NPs ($\text{Fe}_3\text{O}_4@SiO_2$) (magnification of 50 and 100 kx)

In order to test the growth medium composition effect on levan production capability of the isolated *Paenibacillus polymyxa* strain, fermentation processes were carried out in the media containing molasses in varying ratios (Fig. 7a). It was seen that, the product could not be produced due to the lack of sufficient carbon source in the media including 1% of molasses (v/v). When the ratio of molasses in the nutrient media was increased in the range of 5% and 20% (v/v), produced levan concentrations were also boosted significantly due to the increasing available carbon source in the media. However, when the molasses ratio exceeded 20% (v/v), levan concentrations reduced with increased molasses due to the negative effects of the ionic components of molasses on cell membrane activities under studied conditions. Change in levan concentrations in the media at different initial pH values were presented in Fig. 7b. The experimental data clearly showed that, the highest product concentration was reached at the initial pH value of 7.0. Temperature effect on the levan production capacity of the microorganism was tested for both agitated and static processes and the greatest efficiency was obtained in non-agitated system at 37 °C (Fig. 7c). When the variation of the produced levan concentration with time was examined, 54th hour was obtained as optimum due to the maximum levan concentration obtained at that time period (Fig. 7d). As a result, the highest levan concentration of 35.8 g/L was

observed at the 54th hour of the incubation, while the pH and temperature values were 7.0 and 37 °C, respectively, in a static (non-agitated) medium including 20% (v/v) molasses. Conversion efficiency and effective efficiency values were determined as 47.5% and 35.2%. The highest levan concentration obtained with the non-immobilized cells in the medium containing 20% molasses at pH 7, 37 °C, 54th hour was measured as 36.2 g/L.

The results indicated that, there was no significant difference in the maximum levan concentrations obtained with immobilized and non-immobilized cells. This was thought to be related with the nature of the levan-synthesizing enzyme (i.e., levansucrase), which is an extracellular enzyme [57–59]. In the fermentation processes based on intracellular enzymes, the inactive cells are not expected to be involved in the microbial product synthesis due to cell lysis. However, the activity of extracellular enzymes such as levansucrase regardless of whether the cells are living or inactive provides a great advantage in this respect.

Characterization of the Levan Biopolymer

FTIR, NMR and XRD analyzes were performed in order to examine the surface and structural properties of the levan polymer, in addition to antimicrobial and antibiofilm tests.

Fig. 4 TEM micrographs of **a**, **b** untreated magnetite NPs and **c**, **d** silica coated magnetite NPs ($\text{Fe}_3\text{O}_4@\text{SiO}_2$)

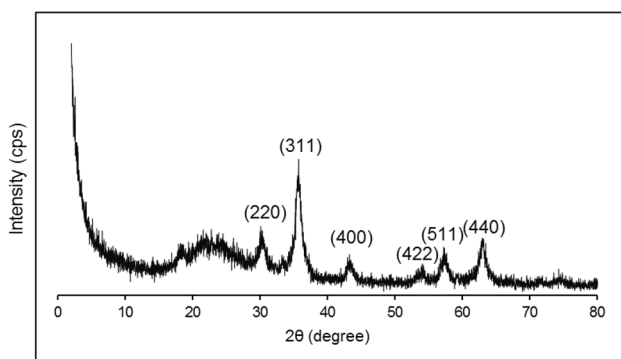
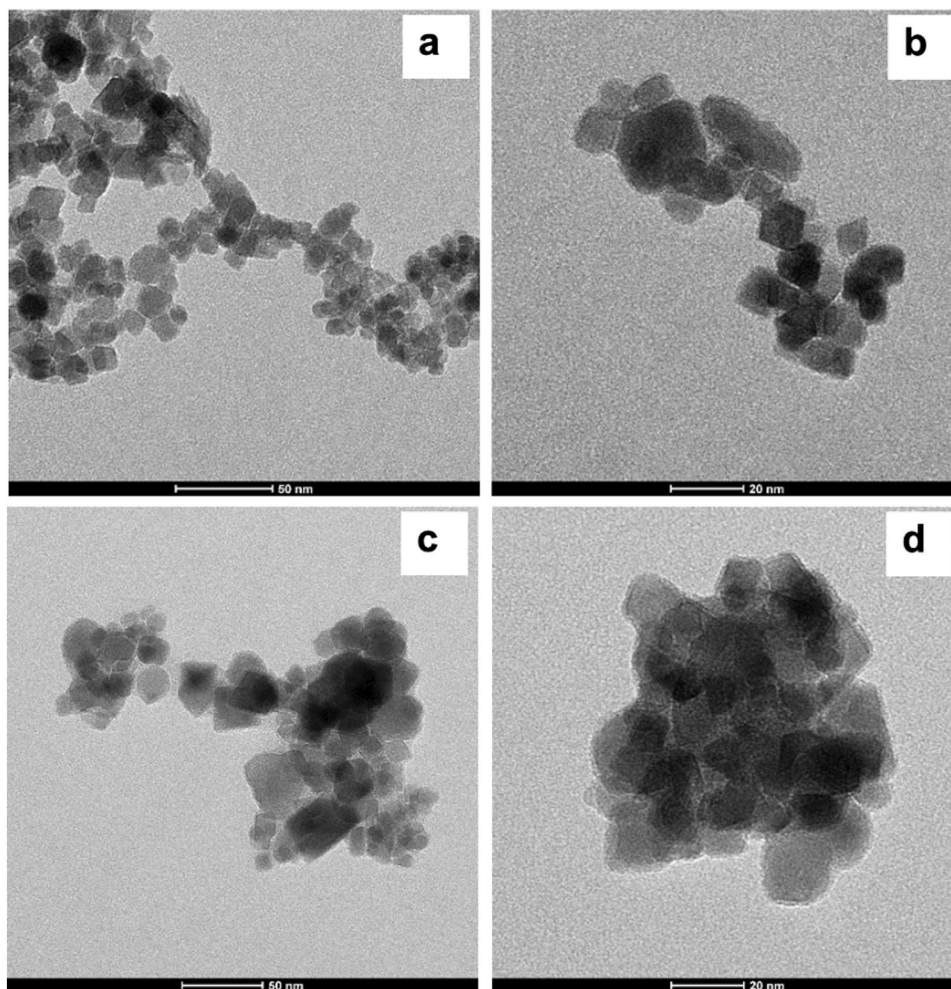


Fig. 5 XRD results of silica coated magnetite NPs ($\text{Fe}_3\text{O}_4@\text{SiO}_2$)

FTIR

The FTIR spectrum of the levan that was produced at optimum conditions was shown in Fig. 8. The peak observed at 3273 cm^{-1} was due to the O–H stretching bond in the polymer, represented the presence of intermolecular hydrogen

bonding. The peaks at 2976 , 2931 and 2877 cm^{-1} indicated the existence of C–H stretching vibration [60]. The band seen at 1636 cm^{-1} was associated with the C=O stretching vibration [14, 61]. The peaks at 1123 and 1012 cm^{-1} were related with the stretching vibration of C–OH groups and stretching vibration of glycosidic C–O–C bonds, which were typical for carbohydrate structures. The peaks at 924 and 808 cm^{-1} revealed symmetric stretching vibration and C–H bending vibration of furanose, respectively [62]. FTIR spectrum of levan biopolymer produced in this study was found to be quite compatible with the ones that were reported in the literature and obtained via various types of microbial species [62–64].

NMR

^{13}C NMR and ^1H NMR analyzes were carried out to confirm the FTIR results of levan biopolymer (Fig. 9). In ^{13}C NMR spectrum, a distinct peak was observed at 104.16 ppm , which was related with C2 signal of β -fructose. The distinctive signals seen at 59.77 , 76.18 , 75.88 , 80.23 and 63.33 ppm

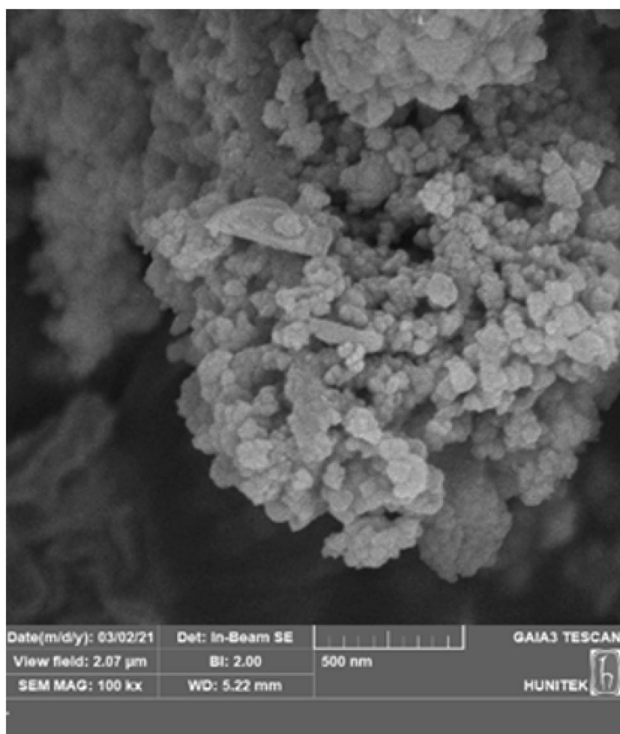


Fig. 6 SEM micrograph of microorganism-immobilized silica coated magnetite NPs composite (Microorganism + $\text{Fe}_3\text{O}_4@ \text{SiO}_2$)

represented the presence of C1, C3, C4, C5 and C6 carbon atoms in the fructose structure, respectively [40, 62]. The chemical shift at 63.33 ppm was accepted as the indicator of β -(2-6) linkage found in C6 of fructose [61]. ^1H NMR analysis also supported the ^{13}C NMR results. The signal at the proton chemical shift of 4.69 ppm was related with D_2O . The distinctive signals were observed between 3.4 and 4.2 ppm range, which was attributed as “ring proton region” and showed the existence of fructose monomer (i.e., the building block of levan biopolymer) [62]. Both ^1H and ^{13}C NMR characteristics of the biosynthesized levan were found to be pretty consistent with the ones reported in the literature [64, 65].

XRD

X-ray diffraction (XRD) analysis was performed to investigate the phase identification and crystallinity properties of the produced levan biopolymer (Fig. 10). A very wide diffraction peak was seen at $2\theta = 18.77$. It was noteworthy that, the interplanetary gap (d spacing) at 18.77 degrees was 4.725 Å and the diffraction peaks were quite significant. These results, which showed the mainly amorphous structure of the biopolymer produced, were quite compatible with the levan characteristics obtained with microbial production in the literature [66, 67].

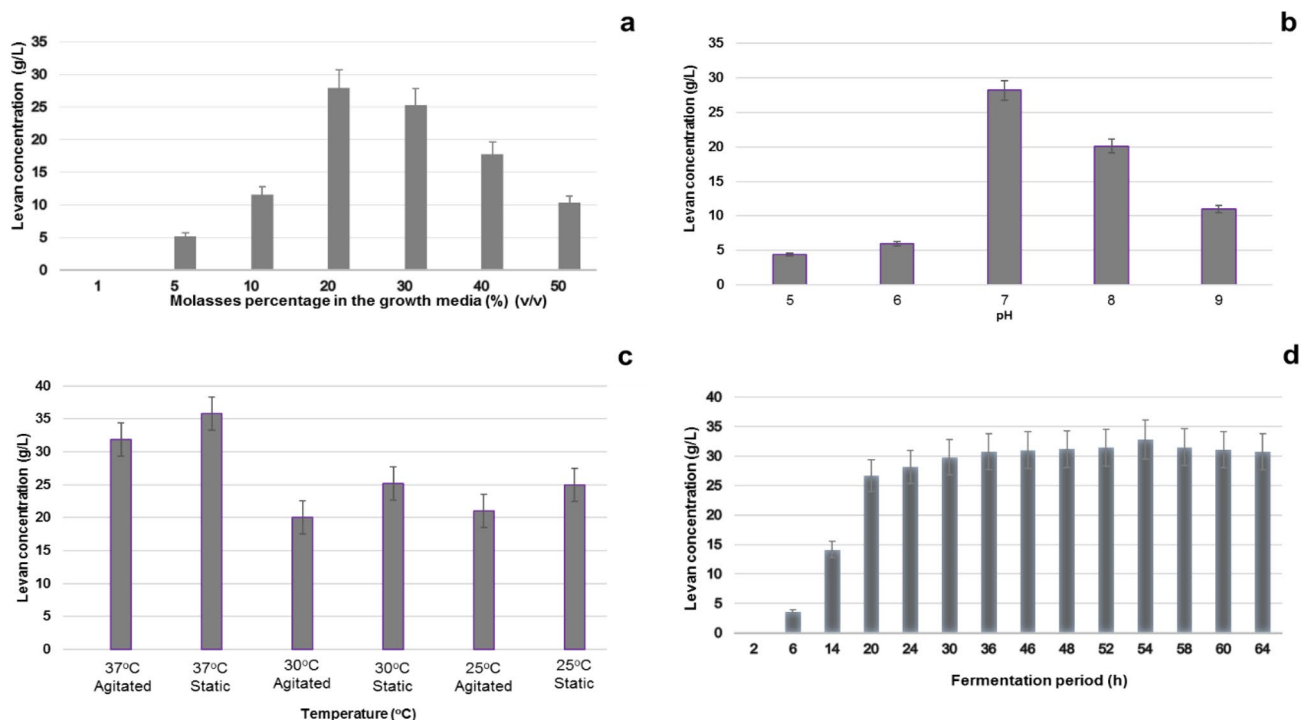


Fig. 7 Effects of molasses percentage in the growth media (a), initial pH (b), temperature (c) and fermentation period (d) on the levan concentration

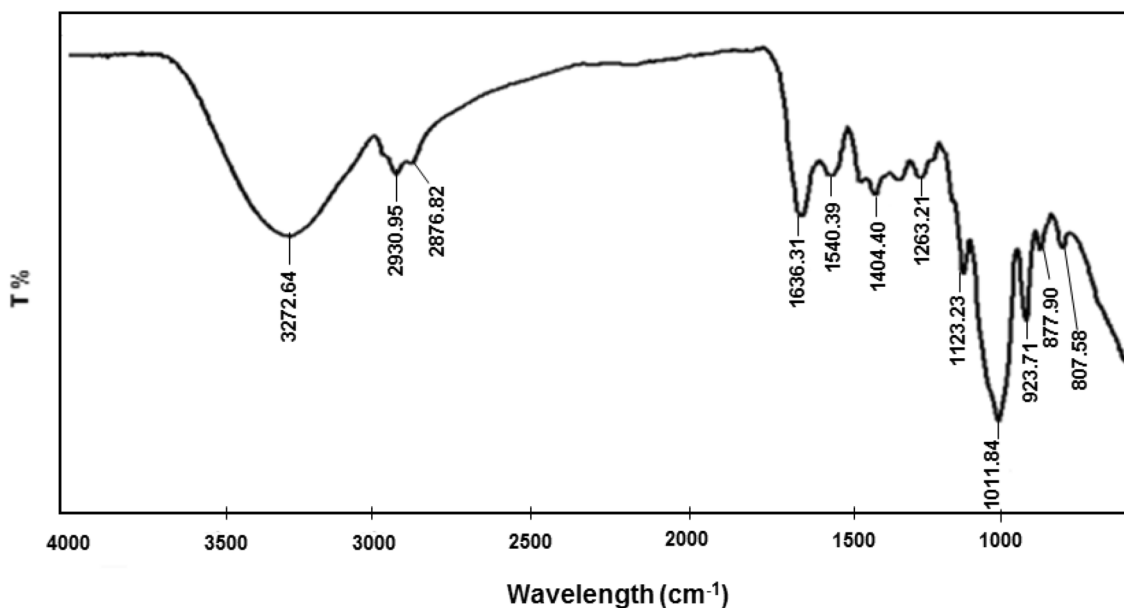


Fig. 8 FTIR spectrum of levan biopolymer produced by *Paenibacillus polymyxa*

Bioactivity of Levan Biopolymer

Antimicrobial Effect

Agar Diffusion Test The antimicrobial effect of the levan obtained by growing *Paenibacillus polymyxa* HCT33-3, which was immobilized on silica-coated iron oxide nanoparticles ($\text{Fe}_3\text{O}_4@\text{SiO}_2$) in molasses medium, was studied on *E.coli* ATCC 35218, *Staphylococcus aureus* subsp *aureus* ATCC®29213™, *Klebsiella pneumoniae* ATCC 1705, *Pseudomonas aeruginosa* ATCC 27853, *Candida albicans* ATCC® 90029™ and *Aspergillus niger* ATCC 6275. Tetracycline (TE, 30 mcg) antibiotic disc was used as a control for bacteria. When the antimicrobial effect of levan synthesized by immobilized cell was evaluated, the proportional decrease in the antimicrobial effect of levan with the decreasing concentration was observed (Table 1). The effectiveness on *Candida albicans* and *Aspergillus niger* than other microorganisms may be due to the fact that these organisms are eukaryotic. Eukaryotic cells have different structures and metabolic pathways from bacterial (prokaryotic) cells. For example, peptidoglycan is structurally different from cell wall components in archaea and unicellular eukaryotes (with the exception of certain plant and algal chloroplasts) and has no homologue in multicellular eukaryotic organisms. Peptidoglycan is a defining feature of the bacterial cell wall and they are identified as targets of beta-lactam antibiotics. The difference in cell structures makes *Candida* and *Aspergillus* more resistant to antimicrobial agents [68, 69]. Shi et al. reported that *Candida albicans* and *Aspergillus niger* cells are more resistant than

Escherichia coli cells, thanks to their eukaryotic cell membrane, and that the inhibition of eukaryotic microorganisms is more difficult [70]. Concentrations of levan lower than 0.5 g/mL was observed to have no effect on growth or killing of *Aspergillus niger*. The antimicrobial effect of the commercially available pure levan produced from *Erwinia herbicola* (Sigma) also showed similar results with the one obtained from the immobilized cells in the study. The highest antimicrobial effect was the 15.5 ± 0.07 mm zone diameter of the levan obtained from immobilized cells at a concentration of 0.50 g/mL, measured on *E. coli* ATCC 35218 strain. In the study of Hamada et al. in 2022, the levan obtained from *Bacillus subtilis* MZ292983.1 strain at a concentration of 0.25 mg/mL was exhibited inhibition zone diameter measured as 8.00 mm on *E.coli* and 10.00 mm on *S.aureus* [14]. Ağçeli et al. reported the antimicrobial effect of 1 g/mL levan obtained from *Pseudomonas mandelii* on *E. coli*, *S. aureus*, *C. albicans* and *A. niger* as 16 mm, 14 mm, 12 mm and 10 mm, respectively [4]. Levan obtained from immobilized cells and free cells did not differ in antimicrobial activity.

Minimum Inhibitory Concentration (MIC) The minimum inhibitory concentration test results given in Table 2 also supported the agar diffusion test. Depending on the decreasing levan concentrations, the antimicrobial effect of levan on microorganisms also decreased. The effect of levan on *A. niger* is very small compared to bacteria. Only 0.5 g/mL levan obtained in the study and pure levan obtained from *Erwinia* showed antimicrobial effect on *A. niger*. In *A. niger* cultures measured as 5.19 ± 0.03 Log CFU/mL as a control,

Fig. 9 ^{13}C NMR (a) and ^1H NMR (b) results of levan biopolymer

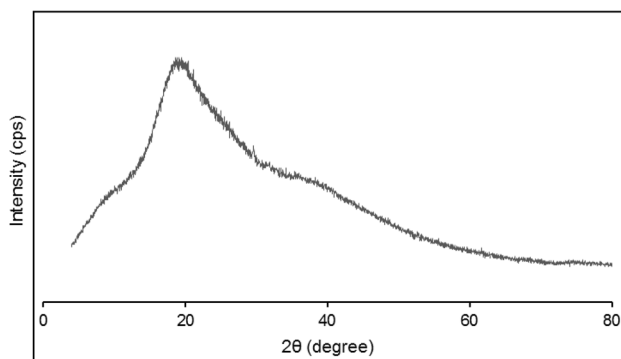
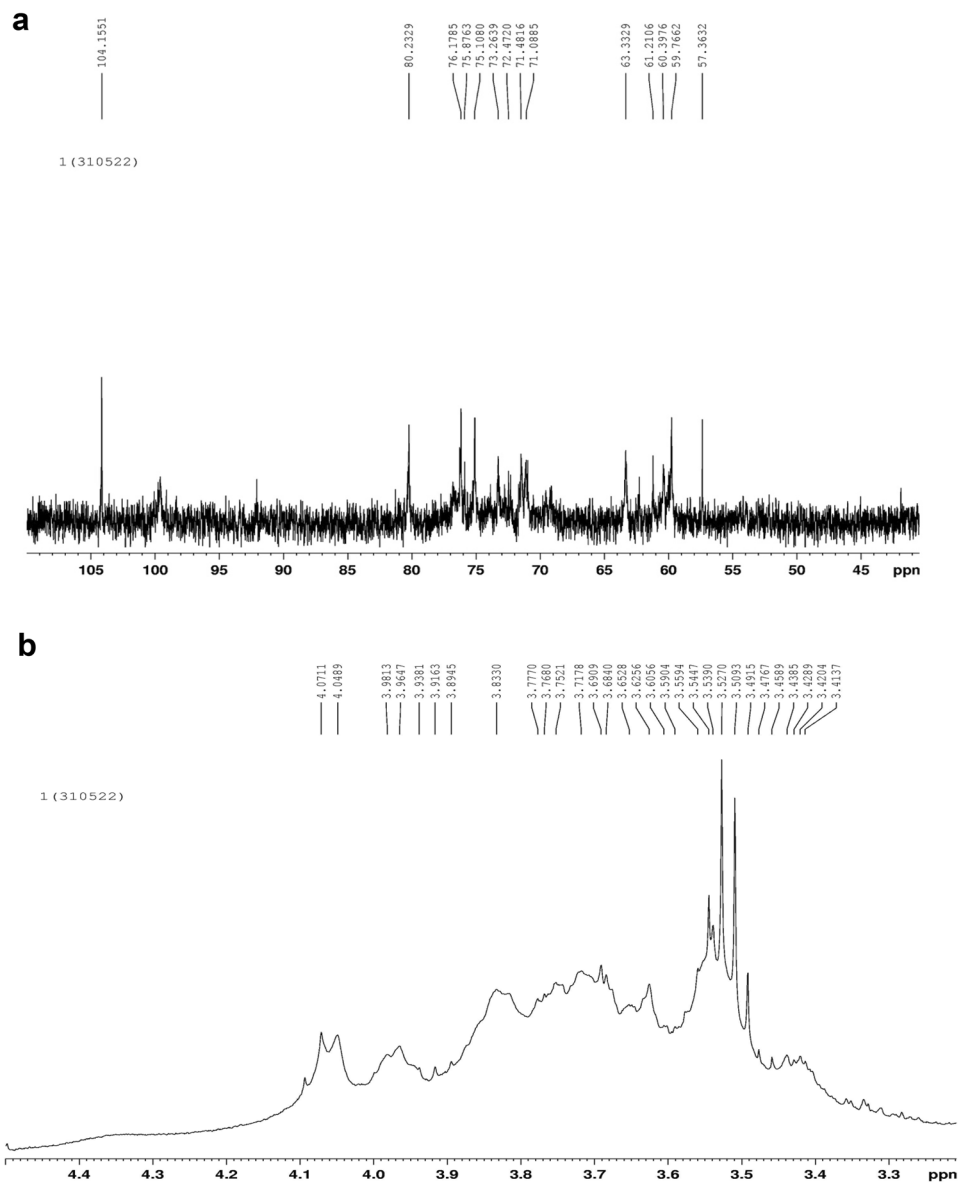


Fig. 10 XRD results of levan biopolymer by immobilized *Paenibacillus polymyxa* HCT33-3

A. niger values measured with 1 g/mL concentration of levan were as 5.02 ± 0.03 and 4.98 ± 0.03 Log CFU/mL, respectively. Contrary to our study, in the study of Gökmen et al. (2020), 0.04 g/mL concentration of levan obtained from *Zymomonas mobilis* showed an antifungal effect on *Aspergillus niger* [49]. For *Candida albicans*, the control value was 8.35 ± 0.05 Log CFU/mL. The 0.5 g/mL concentrations of the levan synthesized in the study decreased the growth with its effect on *Candida albicans* and were measured as 7.96 ± 0.03 and 8.10 ± 0.03 Log CFU/mL, respectively. 0.25 and 0.1 g/mL concentrations of levan from *Paenibacillus polymyxa* HCT33-3 were not effective on *Candida albicans*. When the effect of levan on bacteria was evaluated, all levan concentrations used in the study created an antimicrobial effect on bacteria. With the decreasing levan con-

Table 1 Comparison of antimicrobial effect of levan against different pathogenic microorganisms

| Antimicrobial substance | Inhibition Zone diameters (mm) | | | | | |
|---|--------------------------------|------------------------------|--------------------------------|---------------------------------|---------------------------------|---------------------------|
| | <i>E. coli</i> ATCC 35218 | <i>S. aureus</i> ATCC®29213™ | <i>K. pneumoniae</i> ATCC 1705 | <i>P. aeruginosa</i> ATCC 27853 | <i>C. albicans</i> ATCC® 90029™ | <i>A. niger</i> ATCC 6275 |
| Levan (0.50 g/mL) | 14.5±0.07 | 11.0±0.07 | 11.2±0.07 | 12.3±0.07 | 6.3±0.07 | – |
| Levan (0.25 g/mL) | 11.8±0.07 | 9.0±0.08 | 9.5±0.07 | 10.4±0.07 | – | – |
| Levan (0.10 g/mL) | 7.0±0.03 | 5.7±0.07 | 6.0±0.08 | 6.5±0.07 | – | – |
| Levan (0.50 g/mL) (<i>Erwinia herbicola</i> , Sigma) | 15.0±0.07 | 13.5±0.07 | 13.8±0.07 | 13.7±0.07 | 8.5±0.07 | 7.2±0.07 |
| Levan (0.5 g/mL) (untreated) | 14.0±0.07 | 10.5±0.07 | 11.0±0.07 | 12.5±0.03 | 7.0±0.07 | – |
| Tetracycline (TE, 30 mcg) | 16.5±0.07 | 10.0±0.07 | 18.0±0.09 | 18.0±0.09 | – | – |

Table 2 Comparison of antimicrobial effect with minimum inhibitory concentration of levan obtained from molasses medium on different microorganisms

| Microorganisms | Amount of Levan (g/mL) | | | | | |
|---------------------------------|------------------------|-----------|-----------|-----------|---|-----------------------|
| | Control | 0.5 | 0.25 | 0.1 | 0.5 (<i>Erwinia herbicola</i> , Sigma) | 0.5 Levan (untreated) |
| | (Log CFU/mL) | | | | | |
| <i>E. coli</i> ATCC 35218 | 8.10±0.03 | 7.10±0.03 | 7.55±0.03 | 8.00±0.03 | 6.51±0.03 | 7.05±0.03 |
| <i>S. aureus</i> ATCC®29213™ | 8.23±0.03 | 7.14±0.03 | 7.45±0.03 | 7.97±0.03 | 6.87±0.03 | 7.20±0.03 |
| <i>K. pneumoniae</i> ATCC 1705 | 8.03±0.03 | 7.17±0.05 | 7.58±0.05 | 7.87±0.05 | 6.75±0.03 | 6.83±0.03 |
| <i>P. aeruginosa</i> ATCC 27853 | 8.15±0.03 | 6.82±0.03 | 7.49±0.03 | 7.82±0.03 | 6.74±0.03 | 7.07±0.05 |
| <i>C. albicans</i> ATCC® 90029™ | 8.35±0.05 | 8.10±0.03 | 8.39±0.03 | 8.38±0.03 | 8.00±0.03 | 8.24±0.03 |
| <i>A. niger</i> ATCC 6275 | 5.19±0.03 | 5.17±0.03 | 5.16±0.03 | 5.16±0.03 | 4.98±0.03 | 5.15±0.03 |

concentrations, the effect of levan on bacteria also decreased in direct proportion. Levan from *Lactobacillus gasseri* and levan at concentrations varying between 400 and 1.56 mg/mL were used against *P. aeruginosa* strains isolated from burns and wounds. *Pseudomonas* cultures were inhibited by the obtained pure levan, as well as by certain virulence factors [71].

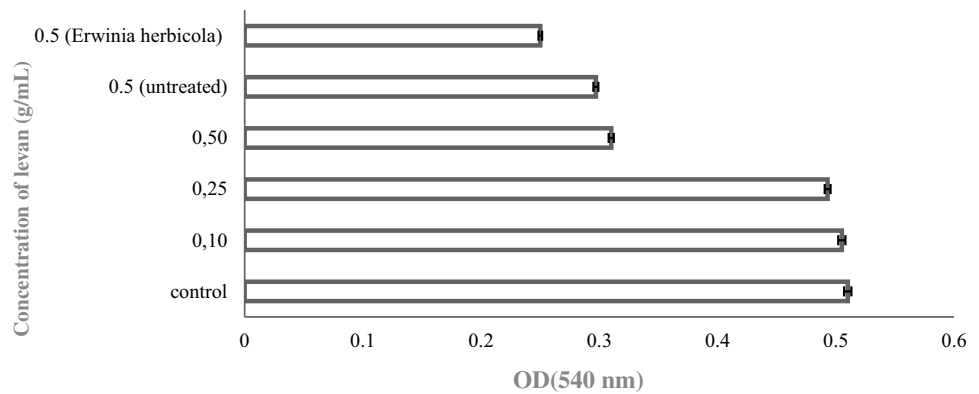
Antibiofilm Effect

The antibiofilm effect of levan obtained by the production of *Paenibacillus polymyxa* HCT33-3 immobilized on silica coated iron oxide nanoparticles ($\text{Fe}_3\text{O}_4@\text{SiO}_2$) in molasses medium was studied on *Pseudomonas aeruginosa* ATCC 27853 strain, which is known to produce biofilms. According to the values measured at 540 nm, the biofilm formation was measured as 0.510 ± 0.03 nm in the control medium without levan, while that OD value decreased to 0.310 ± 0.03 nm in the culture medium incubated with 0.5 g/mL levan (Fig. 11). However, the antibiofilm effect of levan with 0.25 and 0.1 g/mL concentrations on *Pseudomonas* biofilm was measured as 0.493 ± 0.03 and 0.505 ± 0.03 nm, respectively. Considering that these measured values were

the same as the control group, it was determined that levan with concentrations of 0.25 and 0.1 g/mL had no effect on the *Pseudomonas aeruginosa* ATCC 27853 biofilm. In accordance with these results, it was determined that 0.5 g/mL concentrations of levan obtained from molasses medium were effective on *Pseudomonas aeruginosa* ATCC 27853 biofilm. The study results show that the commercially available levan obtained from *Erwinia herbicola* also has antibiofilm effect on the biofilm (0.25 ± 0.03 nm OD) similar to the levan obtained in the study results. The effect of levan produced in molasses medium from non-immobilized cells on *Pseudomonas aeruginosa* ATCC 27853 biofilm was measured as 0.297 ± 0.03 nm OD. There is no significant difference between the data obtained from this result and the levan data obtained from cells immobilized to $\text{Fe}_3\text{O}_4@\text{SiO}_2$ nanoparticles. In molasses medium, the antibiofilm effect of levan obtained with cells immobilized to nanoparticles and levan obtained with free cells is similar.

The results obtained in this study, which reported levan production trajectories of the immobilized and non-immobilized *Paenibacillus polymyxa* HCT33-3 strains comparatively for the first time in the literature, was thought to be bringing a new perspective to the microbial levan production

Fig. 11 Antibiofilm activity of different levan concentrations on *Pseudomonas aeruginosa* ATCC 27853



processes. Although cell immobilization did not have a significant effect on the productivity since the levansucrase is an extracellular enzyme; this process, enabling reusability of this biocomposites, was still considered to be advantageous. This study would form a basis for the future applications targeting low-cost and sustainable production of levan, which is a valuable biopolymer with wide variety of usage.

Conclusion

In the current study, levan production was carried out in molasses medium from *Paenibacillus polymyxa* HCT33-3 strains immobilized on $\text{Fe}_3\text{O}_4@ \text{SiO}_2$ nanoparticles. The efficient levan production in the media including molasses up to 20% by volume showed the sucrose consumption capability of *P. polymyxa* strain. However, more elevated molasses concentrations caused inhibition effect at the conditions studied. 35.8 g/L levan was obtained with the immobilized *P. polymyxa* strain at the optimum conditions. The resulting levan had antimicrobial and antibiofilm properties. Since levansucase is an extracellular enzyme, its activity in both free and immobilized cells is almost the same. The use of waste molasses as a carbon source in biopolymer production and the reuse potential of immobilized microorganisms will encourage low-cost production of levan, an expensive polymer with wide variety of uses. However, further investigation is required to explore the potential reusability of microorganisms immobilized on nanoparticles under various parameters in polymer production, as well as to understand the mechanism of action of levan in both prokaryotic and eukaryotic cells.

Author Contributions GKA and HGY; conceptualization, methodology, software, validation, investigation, resources, data curation, writing—original draft preparation, review and editing.

Funding This study was funded by Hacettepe University Scientific Research Projects Coordination Unit (Project no: FHD-2020-18713).

Data Availability All data generated or analyzed during this study are included in this published article.

Declarations

Conflict of interest The authors declare that they have no known competing financial interests or personal relationships that could have appeared to influence the work reported in this paper.

References

1. Queiroz EAIF, Fortes ZB, da Cunha MAA, Sarilmiser HK, Dekker AMB, Khaper N (2017) Levan promotes antiproliferative and pro-apoptotic effects in MCF-7 breast cancer cells mediated by oxidative stress. *Int J Biol Macromol* 102:565–570. <https://doi.org/10.1016/j.ijbiomac.2017.04.035>
2. Teixeira LCRS, Peixoto RS, Cury JC, Sul WJ, Pellizari VH, Tiedje J, Rosado AS (2010) Bacterial diversity in rhizosphere soil from Antarctic vascular plants of Admiralty Bay, maritime Antarctica. *ISME J* 4(8):989–1001. <https://doi.org/10.1038/ismej.2010.35>
3. Poli A, Kazak H, Gürleyendağ B, Tommonaro G, Pieretti G, Toksoy Öner E, Nicolaus B (2009) High level synthesis of levan by a novel *Halomonas* species growing on defined media. *Carbohydr Polym* 78:651–657. <https://doi.org/10.1016/j.carbpol.2009.05.031>
4. Koşarsoy Ağçeli G, Cihangir N (2020) Nano-sized biopolymer levan: its antimicrobial, anti-biofilm and anti-cancer effects. *Carbohydr Res* 494:108068. <https://doi.org/10.1016/j.carres.2020.108068>
5. Moussa TAA, Al-Qaysi SAS, Thabit ZA, Kadhem SB (2017) Microbial levan from *Brachybacterium phenoliresistens*: characterization and enhancement of production. *Process Biochem* 57:9–15. <https://doi.org/10.1016/j.procbio.2017.03.008>
6. Bouallegue A, Casillo A, Chaari F, La Gatta A, Lanzetta R, Corsaro MM, Bachoual R, Ellouz-Chaabouni S (2020) Levan from a new isolated *Bacillus subtilis* AF17: purification, structural analysis and antioxidant activities. *Int J Biol Macromol* 144:316–324. <https://doi.org/10.1016/j.ijbiomac.2019.12.108>
7. Koşarsoy Ağçeli G, Hammamchi H, Cihangir N (2021) Novel levan/bentonite/essential oil films: characterization and antimicrobial activity. *J Food Sci Technol* 59:249–256. <https://doi.org/10.1007/s13197-021-05009-4>
8. Bahroudi S, Shabanpour B, Combie J, Shabani A, Salimi M (2020) Levan exerts health benefit effect through alteration in bifidobacteria population. *Iran Biomed J* 24:54–59. <https://doi.org/10.29252/ibj.24.1.54>

9. Adamberg K, Tomson K, Talve T, Pudova K, Puurand M, Visnapuu T, Alamäe T, Adamberg S (2015) Levan enhances associated growth of *Bacteroides*, *Escherichia*, *Streptococcus* and *Faecalibacterium* in fecal microbiota. *PLoS ONE* 10(12):e0144042. <https://doi.org/10.1371/journal.pone.0144042>
10. Öner ET, Hernández L, Combie J (2016) Review of Levan polysaccharide: from a century of past experiences to future prospects. *Biotechnol Adv* 34:827–844. <https://doi.org/10.1016/j.biotechadv.2016.05.002>
11. Sturzoiu C, Petrescu M, Galateanu B, Anton M, Nica CI, Simionca G, Dinischiotu A, Stoian G (2011) *Zymomonas mobilis* levan is involved in metalloproteinases activation in healing of wounded and burned tissues. *Sci Pap Anim Sci Biotechnol* 44:453–458
12. Koşarsoy Ağçeli G (2022) Development of ostrich eggshell and nano-levan-based edible biopolymer composite films: characterization and bioactivity. *Polym Bull* 79:11201–11215. <https://doi.org/10.1007/s00289-021-04069-y>
13. Ağçeli GK, Cihangir N (2020) Synthesis, characterization and antimicrobial performance of novel nanostructured biopolymer film based on levan/clay/LL-37 antimicrobial peptide. *Biocatal Agric Biotechnol* 23:101421. <https://doi.org/10.1016/j.bcab.2019.101421>
14. Hamada MA, Hassan RA, Abdou AM, Elsaba YM, Aloufi AS, Sonbol H, Korany SM (2022) Bio-fabricated levan polymer from *Bacillus subtilis* MZ292983.1 with antibacterial, antibiofilm, and burn healing properties. *Appl Sci* 12:1–17. <https://doi.org/10.3390/app12136413>
15. Taylan O, Yilmaz MT, Dertli E (2019) Partial characterization of a levan type exopolysaccharide (EPS) produced by *Leuconostoc mesenteroides* showing immunostimulatory and antioxidant activities. *Int J Biol Macromol* 136:436–444. <https://doi.org/10.1016/j.ijbiomac.2019.06.078>
16. Runyon JR, Nilsson L, Ulmius M, Castro A, Ionescu R, Andersson C, Schmidt C (2014) Characterizing changes in levan physicochemical properties in different pH environments using asymmetric flow field-flow fractionation field-flow fractionation. *Anal Bioanal Chem* 406:1597–1605. <https://doi.org/10.1007/s00216-013-7388-x>
17. Chauhan MK, Varun CS, Samar SK (2011) Life cycle assessment of sugar industry: a review. *Renew Sustain Energy Rev* 15(7):3445–3453. <https://doi.org/10.1016/j.rser.2011.04.033>
18. Kalogiannis S, Iakovidou G, Liakopoulou-Kyriakides M, Kyriakidis DA, Skaracis GN (2003) Optimization of xanthan gum production by *Xanthomonas campestris* grown in molasses. *Process Biochem* 39:249–256. [https://doi.org/10.1016/S0032-9592\(03\)00067-0](https://doi.org/10.1016/S0032-9592(03)00067-0)
19. Yilmaztekin M, Erten H, Cabaroglu T (2008) Production of isoamyl acetate from sugar beet molasses by *Williopsis saturnus* var. *saturnus*. *J Inst Brew* 114:34–38. <https://doi.org/10.1002/j.2050-0416.2008.tb00303.x>
20. Bajaj BK, Singh S, Khullar M, Singh K, Bhardwaj S (2014) Optimization of fibrinolytic protease production from *Bacillus subtilis* I-2 using agro-residues. *Braz Arch Biol Technol*. <https://doi.org/10.1590/S1516-8913201402132>
21. de Moraes Júnior WG, Terrasan CRF, Fernández-Lorente G, Guisán JM, de Resende MM, Pessela BC (2017) Solid-phase amination of *Geotrichum candidum* lipase: ionic immobilization, stabilization and fish oil hydrolysis for the production of Omega-3 polyunsaturated fatty acids. *Eur Food Res Technol* 243:1375–1384. <https://doi.org/10.1007/s00217-017-2848-8>
22. Zhang S, Wang J, Jiang H (2021) Microbial production of value-added bioproducts and enzymes from molasses, a by-product of sugar industry. *Food Chem* 346:128860. <https://doi.org/10.1016/j.foodchem.2020.128860>
23. Nadi A, Melloul M, Boukhriss A, El-Fahime E, Boyer D, Hannache H, Gmouh S (2019) Immobilization of *Bacillus licheniformis* using $\text{Fe}_3\text{O}_4/\text{SiO}_2$ nanoparticles for the development of bacterial bioreactor. *Orient J Chem* 35:854–862. <https://doi.org/10.13005/ojc/350249>
24. Gürmen S, Ebin B (2010) Nanopartiküller ve Üretim Yöntemleri. TMMOB Met Mühendisleri Odası, pp 31–38
25. Mirza S, Ahmad MS, Shah MIA, Ateeq M (2019) Magnetic nanoparticles: drug delivery and bioimaging applications. In: Shah MR, Imran M, Ullah S (eds) *Metal nanoparticles for drug delivery and diagnostic applications*. Elsevier, Amsterdam
26. Materón EM, Miyazaki CM, Carr O, Joshi N, Picciani PHS, Dalmaschio CJ, Davis F, Shimizu FM (2021) Magnetic nanoparticles in biomedical applications: a review. *Appl Surf Sci Adv* 6:100163. <https://doi.org/10.1016/j.apsadv.2021.100163>
27. Faraji AH, Wipf P (2009) Nanoparticles in cellular drug delivery. *Bioorg Med Chem* 17(8):2950–2962. <https://doi.org/10.1016/j.bmc.2009.02.043>
28. Liao H, Nehl CL, Hafner JH (2006) Biomedical applications of plasmon resonant metal nanoparticles. *Nanomedicine* 1(2):201–208. <https://doi.org/10.2217/17435889.1.2.201>
29. Anderson SD, Gwenin VV, Gwenin CD (2019) Magnetic functionalized nanoparticles for biomedical, drug delivery and imaging applications. *Nanoscale Res Lett* 14(1):188. <https://doi.org/10.1186/s11671-019-3019-6>
30. Schwertmann U, Fitzpatrick RW (1992) Iron minerals in surface environments. *Catena Suppl* 21:7–30
31. Liu FM, Zhang Y, Yin W, Hou CJ, Huo DQ, He B, Qian LL, Fa HB (2017) A high-selectivity electrochemical sensor for ultratrace lead (II) detection based on a nanocomposite consisting of nitrogen-doped graphene/gold nanoparticles functionalized with ETBD and $\text{Fe}_3\text{O}_4/\text{TiO}_2$ core-shell nanoparticles. *Sens Actuators B Chem* 242:889–896. <https://doi.org/10.1016/j.snb.2016.09.167>
32. Liu JN, Bu WB, Shi JL (2015) Silica coated upconversion nanoparticles: a versatile platform for the development of efficient theranostics. *Acc Chem Res* 48(7):1797–1805. <https://doi.org/10.1021/acs.accounts.5b00078>
33. Catauro M, Papale F, Roviello G, Ferone C, Bollino F, Trifuoggi M, Aurilio C (2014) Synthesis of SiO_2 and CaO rich calcium silicate systems via sol-gel process: bioactivity, biocompatibility, and drug delivery tests. *J Biomed Mater Res Part A* 102(9):3087–3092. <https://doi.org/10.1002/jbm.a.34978>
34. Tao QL, Li Y, Shi Y, Liu RJ, Zhang YW, Guo J (2016) Application of molecular imprinted magnetic $\text{Fe}_3\text{O}_4/\text{SiO}_2$ nanoparticles for selective immobilization of cellulase. *J Nanosci Nanotechnol* 16(6):6055–6060. <https://doi.org/10.1166/jnn.2016.10853>
35. Reddy PM, Chang KC, Liu ZJ, Chen CT, Ho YP (2014) Functionalized magnetic iron oxide (Fe_3O_4) nanoparticles for capturing gram-positive and gram-negative bacteria. *J Biomed Nanotechnol* 10(8):1429–1439. <https://doi.org/10.1166/jbn.2014.1848>
36. Jang KH, Song KB, Park BS, Kim CH, Chung BH, Choue RW, Lee KS, Lee C, Chun UH, Rhee SK (2001) Levan production by use of the recombinant levansucrase immobilized on titanium-activated magnetite. *Process Biochem* 37(4):339–343. [https://doi.org/10.1016/S0032-9592\(01\)00215-1](https://doi.org/10.1016/S0032-9592(01)00215-1)
37. RCANTicaret (2023) Molasses Properties. <https://rcannakliyat.com>
38. Abou-taleb K, Abdel-Monem M, Yassin M, Draz A (2015) Production, purification and characterization of levan polymer from *Bacillus lentus* V8 strain. *Br Microbiol Res J* 5(1):22–32. <https://doi.org/10.9734/bmrj/2015/12448>
39. Wood IP, Elliston A, Ryden P, Bancroft I, Roberts IN, Waldron KW (2012) Rapid quantification of reducing sugars in biomass hydrolysates: Improving the speed and precision of the dinitrosalicylic acid assay. *Biomass Bioenerg* 44:117–121. <https://doi.org/10.1016/j.biombioe.2012.05.003>
40. Korany SM, El-Hendawy HH, Sonbol H, Hamada MA (2021) Partial characterization of levan polymer from *Pseudomonas*

- fluorescens with significant cytotoxic and antioxidant activity. Saudi J Biol Sci 28(11):6679–6689. <https://doi.org/10.1016/j.sjbs.2021.08.008>
41. Zeng C, Ye G, Li G, Cao H, Wang Z, Ji S (2022) RID serve as a more appropriate measure than phenol sulfuric acid method for natural water-soluble polysaccharides quantification. Carbohydr Polym 28:118928. <https://doi.org/10.1016/j.carbpol.2021.118928>
 42. Kamlage B (1996) Methods for general and molecular bacteriology. Food/Nahrung
 43. Silva SML, Braga CRC, Fook MVL, Raposo CMO, Carvalho LH, Canedo EL (2012) Application of infrared spectroscopy to analysis of chitosan/clay nanocomposites. In: Infrared spectroscopy - materials science, engineering and technology
 44. Hodoroaba VD, Rades S, Salge T, Mielke J, Ortel E, Schmidt R (2016) Characterisation of nanoparticles by means of high-resolution SEM/EDS in transmission mode. IOP Conf 109:012006
 45. Dawn R, Zzaman M, Faizal F, Kiran C, Kumari A, Shahid R, Panatarani C, Joni IM, Verma VK, Sahoo SK, Amemiya K, Singh VR (2022) Origin of magnetization in silica-coated Fe₃O₄ nanoparticles revealed by soft X-ray magnetic circular dichroism. Braz J Phys 52:99. <https://doi.org/10.1007/s13538-022-01102-x>
 46. Glaria A, Soulé S, Hallali N, Ojo WS, Mirjolet M, Fuks G, Cornejo A, Allouche J, Dupin JC, Martinez H, Carrey J, Chaudret B, Delpech F, Lachaize S, Nayral C (2018) Silica coated iron nanoparticles: synthesis, interface control, magnetic and hyperthermia properties. RSC Adv 8(56):32146–32156. <https://doi.org/10.1039/c8ra06075d>
 47. Biro SJ, Özkul İ (2018) Zn_{0.4}Cd_{0.4} Composite fabrication and characterization. Selcuk Univ J Eng Sci Technol. <https://doi.org/10.15317/scitech.2018.143>
 48. Guzińska K, Kaźmierczak D, Dymel M, Pabjańczyk-Wlazło E, Boguń M (2018) Anti-bacterial materials based on hyaluronic acid: selection of research methodology and analysis of their antibacterial properties. Mater Sci Eng C 93:800–808. <https://doi.org/10.1016/j.msec.2018.08.043>
 49. Gokmen GG, Silbir S, Goksungur Y, Kisla D (2020) The effect of microbial levan on the growth of microorganisms: inhibitory or stimulatory? Fresenius Environ Bull 29(03):1648–1654
 50. Silbir S, Dagbagli S, Yegin S, Baysal T, Goksungur Y (2014) Levan production by *Zymomonas mobilis* in batch and continuous fermentation systems. Carbohydr Polym 99:454–461. <https://doi.org/10.1016/j.carbpol.2013.08.031>
 51. Nalbandian L, Patrikiadou E, Zaspalis V, Anna P, Eleana H, Christos NP (2015) Magnetic nanoparticles in medical diagnostic applications: synthesis, characterization and proteins conjugation. Curr Nanosci 12(4):455–468. <https://doi.org/10.2174/1573413712666151210230002>
 52. Chaki SH, Malek TJ, Chaudhary MD, Tailor JP, Deshpande MP (2015) Magnetite Fe₃O₄ nanoparticles synthesis by wet chemical reduction and their characterization. Adv Nat Sci Nanosci Nanotechnol. <https://doi.org/10.1088/2043-6262/6/3/035009>
 53. Izza Taib N, Pierre TG, Woodward RC, House MJ (2019) Magnetic properties of magnetite nanoparticles (Fe₃O₄-NPs) coated with mesoporous silica by surfactant templated sol-gel method. Int J Eng Technol 7:533. <https://doi.org/10.14419/ijet.v7i4.14.27785>
 54. Karimi Pasandideh E, Kakavandi B, Nasserli S, Mahvi AH, Nabizadeh R, Esrafil A, Kalantary RR (2016) Silica-coated magnetite nanoparticles core-shell spheres (Fe₃O₄@SiO₂) for natural organic matter removal. J Environ Heal Sci Eng 14:21. <https://doi.org/10.1186/s40201-016-0262-y>
 55. Ouyang ZW, Chen EC, Wu TM (2015) Thermal stability and magnetic properties of polyvinylidene fluoride/magnetite nanocomposites. Materials (Basel) 8(7):4553–4564. <https://doi.org/10.3390/ma8074553>
 56. Nicola R, Costișor O, Ciopec M, Negrea A, Lazău R, Ianăși C, Picioruș EM, Len A, Almásy L, Szerb EI, Putz AM (2020) Silica-coated magnetic nanocomposites for Pb²⁺ removal from aqueous solution. Appl Sci 10(8):2726. <https://doi.org/10.3390/AP10082726>
 57. Li H, Schenk A, Srivastava A, Zhurina D, Ullrich MS (2006) Thermo-responsive expression and differential secretion of the extracellular enzyme levansucrase in the plant pathogenic bacterium *Pseudomonas syringae* pv. glycinea. FEMS Microbiol Lett 265(2):178–185. <https://doi.org/10.1111/j.1574-6968.2006.00486.x>
 58. Thakham N, Thaweesak S, Teerakulkittipong N, Traiosot N, Kakaew A, Lirio GAC, Jangiam W (2020) Structural characterization of functional ingredient levan synthesized by *Bacillus siamensis* isolated from traditional fermented food in Thailand. Int J Food Sci 6:1–12. <https://doi.org/10.1155/2020/7352484>
 59. Jakob F, Gebrande C, Bichler RM, Vogel RF (2020) Insights into the pH-dependent, extracellular sucrose utilization and concomitant levan formation by *Gluconobacter albidus* TMW 2.1191. Antonie van Leeuwenhoek. Int J Gen Mol Microbiol 113:863. <https://doi.org/10.1007/s10482-020-01397-3>
 60. Yu X, Li L, Zhang J, Shen Z, Zhu C, Wang P, Jiang X (2016) Structural analysis of macromolecular levan produced by *Bacillus megaterium* GJT321 based on enzymatic method. Int J Biol Macromol 93(Part A):1080–1089. <https://doi.org/10.1016/j.ijbmac.2016.09.086>
 61. Mamay WD, Hertadi R (2015) Isolation and characterization of levan from moderate halophilic bacteria *Bacillus licheniformis* BK AG21. Procedia Chem 16:292–298. <https://doi.org/10.1016/j.proche.2015.12.055>
 62. Wang J, Xu X, Zhao F, Yin N, Zhou Z, Han Y (2022) Biosynthesis and structural characterization of levan by a recombinant levansucrase from *Bacillus subtilis* ZW019. Waste Biomass Valoriz 13:4599–4609. <https://doi.org/10.1007/s12649-022-01814-w>
 63. Jathore NR, Bule MV, Tilay AV, Annapure US (2012) Microbial levan from *Pseudomonas fluorescens*: characterization and medium optimization for enhanced production. Food Sci Biotechnol 21:1045–1053. <https://doi.org/10.1007/s10068-012-0136-8>
 64. Al-Qaysi SAS, Al-Haideri H, Al-Shimmary SM, Abdulhameed JM, Alajrawy OI, Al-Halbosiy MM, Moussa TAA, Farahat MG (2021) Bioactive levan-type exopolysaccharide produced by *Pantoea agglomerans* ZMR7: characterization and optimization for enhanced production. J Microbiol Biotechnol 31(5):696–704. <https://doi.org/10.4014/jmb.2101.01025>
 65. Oktavia I, Fithriah AN, Permatasari NU, Ratnaningsih E, Hertadi R (2020) Levan produced by the halophilic bacterium *Bacillus licheniformis* BK1 as a nanoparticle for protein immobilization. Indones J Chem. <https://doi.org/10.22146/ijc.41064>
 66. Mohite BV, Koli SH, Rajput JD, Patil VS, Agarwal T, Patil SV (2019) Production and characterization of multifacet exopolysaccharide from an agricultural isolate, *Bacillus subtilis*. Biotechnol Appl Biochem 66:1010–1023. <https://doi.org/10.1002/bab.1824>
 67. Xu W, Liu Q, Bai Y, Yu S, Zhang T, Jiang B, Mu W (2018) Physicochemical properties of a high molecular weight levan from *Brenneria* sp. EniD312. Int J Biol Macromol 109:810–818. <https://doi.org/10.1016/j.ijbiomac.2017.11.056>
 68. Otten C, Brilli M, Vollmer W, Viollier PH, Salje J (2018) Peptidoglycan in obligate intracellular bacteria. Mol Microbiol 107(2):142–216. <https://doi.org/10.1111/mmi.13880>
 69. Garde S, Chodiseti PK, Reddy M (2021) Peptidoglycan: structure, synthesis, and regulation. EcoSal Plus. <https://doi.org/10.1128/ecosalplus.esp-0010-2020>
 70. Shi L, Zhao Y, Zhang X, Su H, Tan T (2008) Antibacterial and anti-mildew behavior of chitosan/nano-TiO₂ composite emulsion. Korean J Chem Eng 25:1434–1438. <https://doi.org/10.1007/s11814-008-0235-7>
 71. Zainulabdeen SMS, Abdul J, Salmanand S, Khalaf K (2021) Purification and characterization of levan from *Lactobacillus*

gasseri and its effect against *Pseudomonas aeruginosa*. NVEO 8(4):5788–5808

Publisher's Note Springer Nature remains neutral with regard to jurisdictional claims in published maps and institutional affiliations.

Springer Nature or its licensor (e.g. a society or other partner) holds exclusive rights to this article under a publishing agreement with the author(s) or other rightsholder(s); author self-archiving of the accepted manuscript version of this article is solely governed by the terms of such publishing agreement and applicable law.